CFD prediction of mean flow, power number, mixing time and just suspended speed in mixing tank

Chin Cai Chia[1], *Zhi Lei* Wang[2], *Vidhya* Rajagopal[3], and *Jolius* Gimbun[2,4*]

[1]Faculty of Chemical and Process Engineering Technology, Universiti Malaysia Pahang Al-Sultan Abdullah, Gambang 26300, Pahang, Malaysia
[2]Centre for Research in Advanced Fluid and Processes (Fluid Centre), Universiti Malaysia Pahang Al-Sultan Abdullah, Gambang 26300, Pahang, Malaysia
[3]Department of Biotechnology, Faculty of Science & Humanities, SRM Institute of Science and Technology, Ramapuram, Chennai 600089, Tamil Nadu, India
[4]Department of Biotechnology, Saveetha School of Engineering, Saveetha Institute of Medical and Technical Sciences, Chennai 602105, Tamil Nadu, India

Abstract. Efficient multiphase mixing in stirred tanks is essential for chemical, pharmaceutical, and food processes. This study examines the relationship between power number (N_{Po}), just-suspended speed (N_{js}), and mixing time to improve energy efficiency and suspension performance. Computational fluid dynamics (CFD) simulations were performed in ANSYS Fluent for a fully baffled, flat-bottom tank fitted with a down-pumping six-bladed pitched-blade turbine. The Reynolds-Averaged Navier–Stokes (RANS) turbulence model, multiple reference frame (MRF) approach, and discrete phase model (DPM) were applied to characterize fluid flow and solid–liquid interactions. Predicted impeller power numbers and mixing times agreed with published experimental data, with an average deviation of about 6.0%. However, the prediction of N_{js} remained challenging, even when power draw, mixing time, and flow field were reproduced with reasonable accuracy. Therefore, caution is advised when predicting solid–liquid dispersion in stirred tanks.

1 Introduction

Effective mixing in stirred tanks is critical in chemical, pharmaceutical, and food industries, where they are widely applied to enhance mass transfer, heat transfer, and chemical reaction rates. In many of these applications, the processes involve multiphase mixing, in which solid–liquid interactions play a decisive role in determining energy efficiency, product homogeneity, and overall process quality. Consequently, a thorough understanding of the interplay between power input, fluid flow patterns, and particle suspension behavior is essential for the proper design, scale-up, and operation of stirred tanks [1]. To evaluate mixing performance, several key indicators are commonly employed, including the power

* Corresponding author: jolius@umpsa.edu.my

number (N_{Po}), the just-suspended impeller speed (N_{js}), and the characteristic mixing time, each of which provides valuable insight into hydrodynamic performance and suspension efficiency.

Computational fluid dynamics (CFD) has been extensively used to predict mixing time in mixing tanks by simulating tracer transport, flow field and turbulent flows. For instance, Li and Xu [2] performed a CFD simulation of stirred tank driven by a dual six-blade Rushton turbine. They found that feeding point location and impeller spacing significantly affect mixing, with global mixing times being insensitive to impeller speed once in fully turbulent conditions. Ochieng and Onyango [3] combined experimental measurements via laser doppler velocimetry and CFD to study stirred tanks with and without draft tubes. They found reasonable agreement between CFD and experiments. They concluded that inclusion of draft tubes reduced the energy required for homogenization by ~17–19%. More recently, Reid et al. [4] evaluated the effect of the size of the moving zone (impeller region) used during CFD simulation of a Rushton turbine tank. They reported that the moving zone diameter may affect the prediction of mixing time.

CFD can be used to predict the N_{js} of solid–liquid suspensions in stirred tanks. However, its accuracy depends strongly on modeling choices and particle representation. Tamburini et al. [5], for instance, showed that CFD can predict the cloud height of solids to represent the 'just-suspension' criterion in stirred tanks. CFD predictions are known to be sensitive to the turbulence model, numerical setup, and multiphase approach (Eulerian–Eulerian, Eulerian–Lagrangian, or particle-resolved) [6]. Particle shape and orientation markedly affect drag, settling, and therefore N_{js}. Hence, assuming spherical particle shapes often underpredicts the required speed unless corrections are made [7]. The recommended best practice is to validate simulations against experimental N_{js} or cloud-height data and, where feasible, to include shape effects or apply empirical correction factors to improve CFD prediction accuracy [8].

Despite their broad application, optimizing mixing efficiency remains challenging, as energy consumption and performance depend on tank geometry, impeller design, and operating conditions. CFD has emerged as a powerful tool for analyzing these factors, providing insights into fluid flow and particle suspension beyond experimental limitations [9]. Most previous studies have focused on either mixing time or N_{js}, with limited work combining both. In this study, CFD was used to predict the power number, mixing time, and N_{js} of a stirred tank driven by a pitched-blade impeller, with the aim of investigating how the prediction of mixing time may influence the prediction of N_{js}, and vice versa.

2 Methodology

2.1 Tank geometry and configuration

Figure 1 shows the stirred tank geometry used in this work. The tank is a fully baffled, flat-bottom cylindrical vessel with diameter T = 0.7 m and liquid height H = T, giving an industrially common H/T = 1 ratio. Four vertical baffles of width B = T/10 are symmetrically placed to suppress swirling and enhance mixing. Mixing is driven by a down-pumping six-bladed pitched blade turbine (PBTD-6) with diameter D = 0.2 m (D/T = 0.29), mounted at a clearance C = T/3 from the bottom for effective flow distribution and solids suspension. The working fluid is a tap water ($\rho l = 1000$ kg/m³), and the solid phase consists of glass beads (dp =150 μm, $\rho s = 2500$ kg/m³) at a loading of 7% v/v, as in Sardeshpande et al. [10].

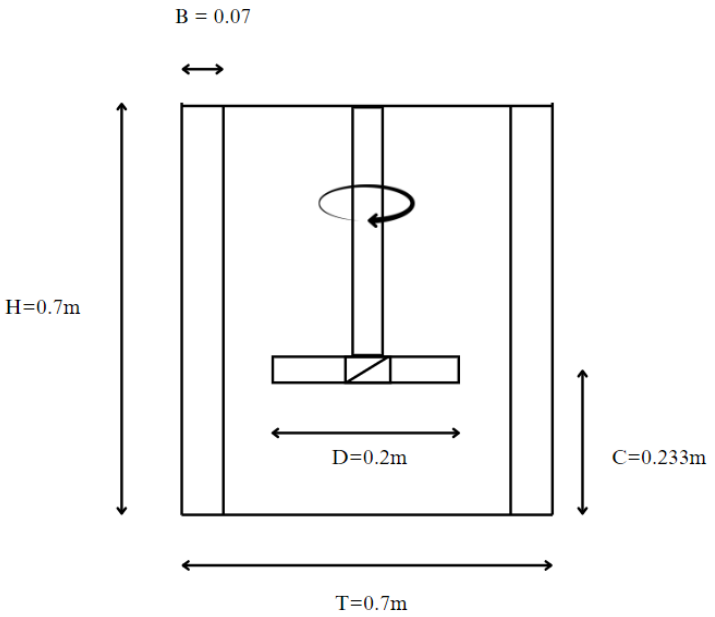

Fig. 1. Stirred tank geometry and configuration.

2.2 CFD simulation

The turbulence modelling was modelled using the realizable k–ε model which provides an improved prediction over the standard k–ε model as they account for strain and rotation effects more accurately [11]. According to Gimbun et al. [12], the improvement in prediction is attributed to the introduction of a new turbulent viscosity formulation. The transport equation model for k and ε were given as follows:

$$\frac{\partial \rho k}{\partial t} + \frac{\partial}{\partial x_i}(\rho u_i k) = \frac{\partial}{\partial x_i}\left[\left(\mu + \frac{\mu_t}{\sigma_k}\right)\frac{\partial k}{\partial x_i}\right] + \rho P_k - \rho\varepsilon \tag{1}$$

$$\frac{\partial \rho \varepsilon}{\partial t} + \frac{\partial}{\partial x_i}(\rho \varepsilon u_i) = \frac{\partial}{\partial x_i}\left[\left(\mu + \frac{u_t}{\sigma_\varepsilon}\right)\frac{\partial \varepsilon}{\partial x_i}\right] + \rho C_1 S\varepsilon - \rho C_2 \frac{\varepsilon}{k + \sqrt{v\varepsilon}} + C_{1\varepsilon}\frac{\varepsilon}{k} G_b C_{3\varepsilon} \tag{2}$$

where,

$$C_1 = \max\left[0.43, \frac{\eta}{\eta + 5}\right] \tag{3}$$

The relation for the turbulent viscosity, μ_t, and turbulent production, P_k, in realizable $k - \varepsilon$ model is computed by:

$$\mu_t = \rho C_\mu \frac{k^2}{\varepsilon} \tag{4}$$

$$P_k = \mu_t \left(\frac{\partial u_j}{\partial x_i} + \frac{\partial u_i}{\partial x_j} \right) \frac{\partial u_j}{\partial x_i} \tag{5}$$

The C_μ is no longer constant for realizable k–ε model, instead it was computed from $C_\mu = 1/(A_0 + A_s\, kU^*/\varepsilon)$. The values of the model constants are: $C_{1\varepsilon}$ = 1.44, C_2 = 1.9, σ_ε = 1.2 and σ_k = 1.

Solid dispersion was modelled using discrete phase model (DPM). In DPM, the trajectory of the discrete phase particle is predicted by integrating force balance on the particle, which is also known as Lagrangian reference frame. The particle inertia with the forces exerted on the particle is given by:

$$\frac{du_p}{dt} = F_D(u - u_p) + \frac{g_x(\rho_p - \rho)}{\rho_p} + F_x \tag{6}$$

where drag force, $F_{D,}$ is given by eq. (7) as function to particle Reynolds number, Re_p. The drag coefficient, C_D, for spherical particle is given as follows:

$$F_D = \frac{18\mu}{\rho_d d_d^2} \frac{C_D R_{e_p}}{24} \tag{7}$$

$$C_D = a_1 + \frac{a_2}{R_{e_p}} + \frac{a_3}{Re_p^2} \tag{8}$$

A computational grid containing cells ranging from 354488 to 710133 was prepared using ANSYS Meshing. The mesh consists of high-quality tetrahedral and polyhedral elements, with an orthogonal quality greater than 0.26 and an equiangle skew below 0.5. Moreover, the y^+ values range from about 2 to 124, which is adequate for the standard k-ε model, as it accepts y^+<300. The grid refinement was made in the impeller region where the turbulent flow is most intense (Figure 2).

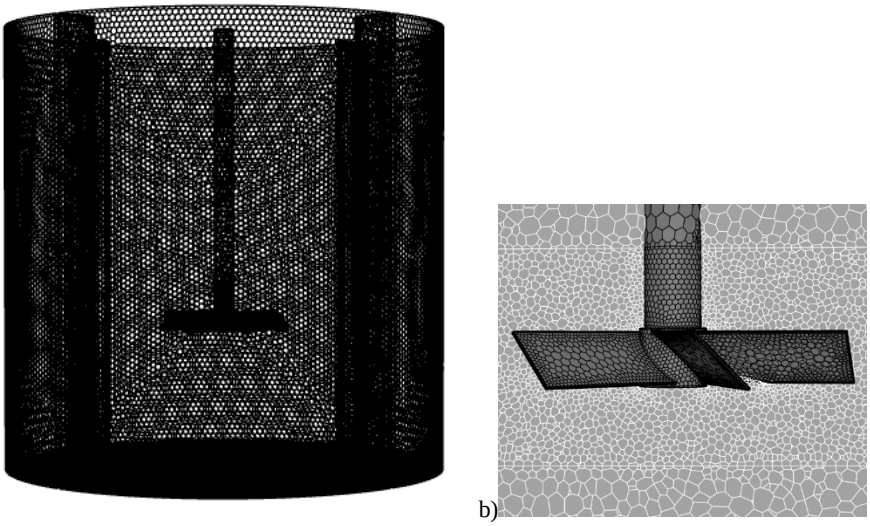

a) b)

Fig. 2. a) Computational grid for the tank, b) Grid refinement at the impeller zone.

The impeller rotation was modeled using the multiple reference frame method in ANSYS Fluent 18.2. Momentum and turbulence were discretized using a second-order discretization

scheme, while pressure was set using the pressure staggered option. The simulation was considered converged once the residuals fell below 1×10^{-3}. The CFD simulations were made on an HP Z220 workstation equipped with Intel Xeon 3.2 GHz processor and 16 GB of RAM.

Grid dependent study was performed to ensure that the grid used for the simulation has adequate grid density. Three different grid densities designated as coarse (354488 cells), intermediate (549218 cells) and fine (710133 cells) was studied and the prediction using the aforesaid grid was compared. It was found that the intermediate ($N_{Po} = 1.60$) and fine ($N_{Po} = 1.72$) grid yielded almost similar value to that of experimental measurement by Sardeshpande et al. [10], $N_{Po} = 1.68$ at $Re = 1 \times 10^5$. Therefore, in the interest of reducing the computational requirements, the intermediate grid was chosen for the remainder of this work.

3 Results and discussion

3.1 Fluid flow and particle tracking

A pitched blade impeller is widely used in stirred tanks because it can generate both axial and radial flow, making it versatile for multipurpose mixing operations. The pitched blade impeller produces a mixed flow pattern dominated by axial circulation with a supplementary radial component. This flow structure promotes efficient bulk mixing, good solid suspension, and moderate shear, making it a versatile choice for many industrial mixing processes.

Figure 3 shows the CFD prediction of velocity vector driven by PBTD-6 featuring a downward flow at the tip of the impeller, which then circulate upward near the tank wall towards the tank surface and moving down around the impeller shaft. At the bottom of the tank, a weak secondary recirculation can be observed. This flow feature from PBTD-6 is similar to those reported by Ge et al. [13].

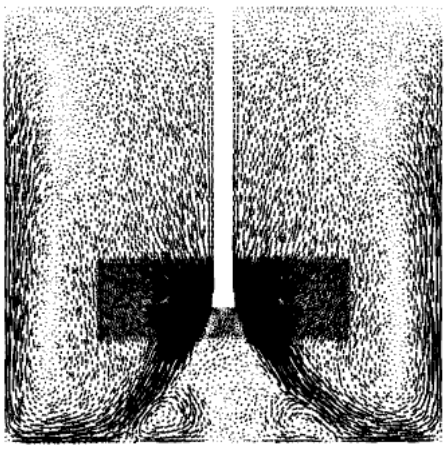

Fig. 3. Predicted vector plot.

Figure 4 shows the contour of velocity magnitude normalised by impeller tip speed, V_{tip}. Trindade Koyro et al. [14] performed a PIV measurement of similar tank configuration, i.e., stirred tank agitated by PBTD-6 with bottom clearance of T/3. They reported a peak velocity magnitude of $0.55V_{tip}$ just below the impeller blade at z/H = 0.27. In this work, the peak velocity magnitude at z/H = 0.27 is about $0.57V_{tip}$, which is in close agreement to that of Trindade Koyro et al. [14] experimental measurement. The good prediction of the mean velocity implies that the CFD simulation is done correctly and can be used to study fluid mixing and solid dispersion.

Figure 5 shows the particle tracking in the stirred tank at impeller speed of 150 and 600 RPM. It can be observed, that at this impeller speed particles are mostly adequately suspended with no evidence of particle sedimenting on the tank bottom. Although, it was observed that particles in the tank agitated at 150 RPM tends to disperse at the bottom at around the impeller.

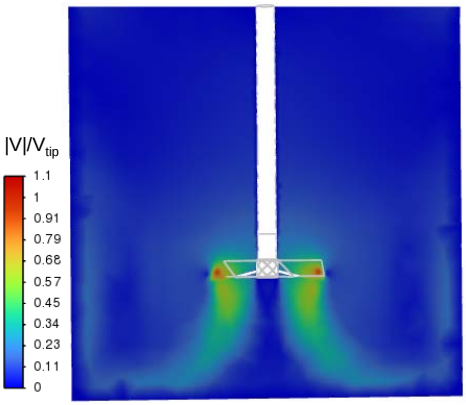

Fig. 4. Prediction of velocity magnitude.

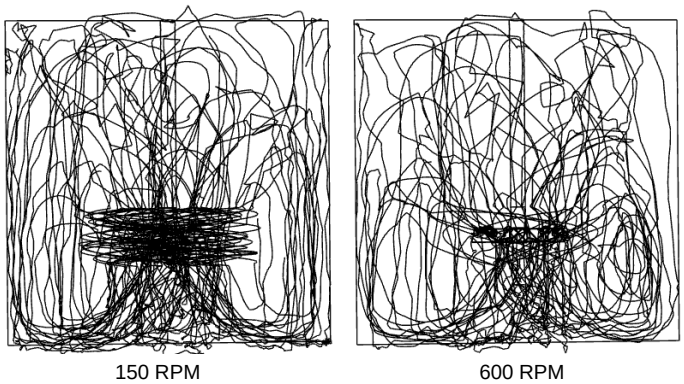

Fig. 5. Particle tracking at 150 and 600 RPM.

3.2 Prediction of power number

Table 1 presents the predicted power number, N_{po}, obtained from the CFD simulations and compares it with the experimental measurements reported by Sardeshpande et al. [10]. The CFD prediction demonstrates good agreement with the published experimental data, with a deviation of approximately 6%. For reference, the turbulent power number commonly reported for pitched blade impellers lies in the range of 1.2–1.7 [1].

It is well established that impeller geometry, particularly blade thickness, can influence the measured power number [15]. However, the exact impeller thickness used in Sardeshpande et al. [10] was not specified. In the present study, the blade thickness was therefore assumed to be 2 mm. Although variations in thickness are known to affect N_{Po}, the impact is generally modest for pitched blade impellers [16].

Given these considerations, the CFD-predicted N_{Po} in this work is regarded as acceptable. Moreover, it provides a reliable basis for estimating key performance indicators of the stirred tank, such as mixing time, where accurate values of power input per unit volume are essential.

Table 1. Prediction of power number

Re	N (RPM)	N_{Po}		Deviation
		This work	**Sardeshpande et al.** [10]	
100000	150	1.60	1.68	4.7%
133000	200	1.59	1.50	6.0%

3.3 Prediction of mixing time

Mixing time is a key performance parameter in stirred tanks because it directly influences process efficiency, product quality, and scale-up reliability. Mixing time is important because it links hydrodynamics (impeller design, power input) to process performance (reaction rate, yield, and product uniformity.

Figure 6 presents the CFD-predicted mixing time as a function of impeller speed. The predictions show good agreement with the experimental measurements reported by Sardeshpande et al. [10] and Kuzmanic et al. [17]. The discrepancy observed relative to Sardeshpande et al. [10] is likely attributed to minor deviations in the predicted power number (N_{Po}), which was used in the mixing time calculation. It is noteworthy that the stirred tank and impeller dimensions in this study are identical to those in Sardeshpande et al. [10]. In contrast, Kuzmanic et al. [17] employed a four-blade pitched blade impeller, whereas the present work used a six-blade configuration. Thus, despite employing the same impeller type, the difference in blade number may account for the observed deviation.

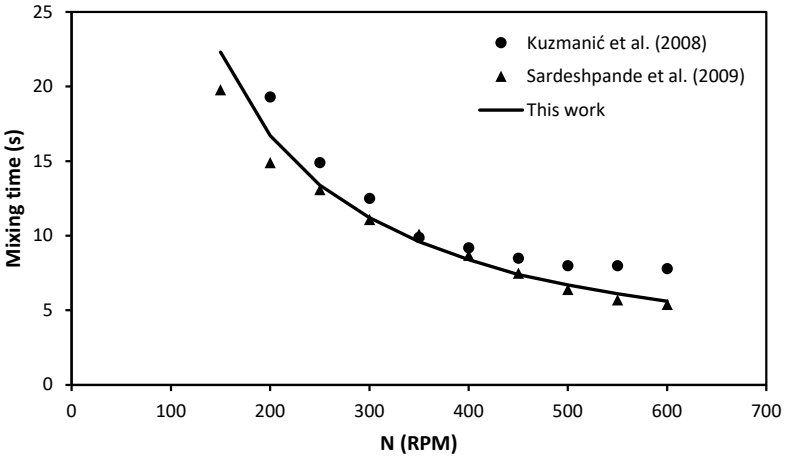

Fig. 6. Prediction of mixing time against published experimental data.

3.4 Prediction of just suspended impeller speed

The impeller just-suspended speed is one of the most important design and operating parameters in solid–liquid mixing. The just-suspended speed is important because it provides a practical benchmark for achieving complete solid suspension with minimum energy input, ensuring both process efficiency and product quality.

Figure 7 presents the predicted just-suspended impeller speed (N_{js}) in comparison with the experimental data reported by Sardeshpande et al. [10]. A noticeable deviation can be observed between the CFD predictions and the measured experimental values, indicating a limitation in the modeling approach. One of the primary sources of this discrepancy is the assumption of perfectly spherical particles within the CFD simulations. In reality, particles encountered in experimental systems are rarely ideal spheres; instead, they often display irregular, oblate, or elliptical morphologies.

Particle shape exerts a strong influence on the hydrodynamic behavior of the suspension, particularly by altering the drag force experienced by the particles and their settling tendencies. Such variations in morphology also affect particle–fluid interactions and the overall efficiency of solid dispersion, both of which play a critical role in determining N_{js}. In this case, the simulations underpredict the experimental N_{js} values, suggesting that the modeled system requires less impeller power to achieve just suspension than what is actually needed in practice.

If uncorrected, this underprediction can mislead the design process, resulting in stirred tank configurations that are inadequate for proper solid–liquid dispersion. Hence, incorporating more realistic particle shape representations or appropriate correction factors into CFD models is essential for improving the accuracy of N_{js} predictions and ensuring reliable scale-up of mixing operations.

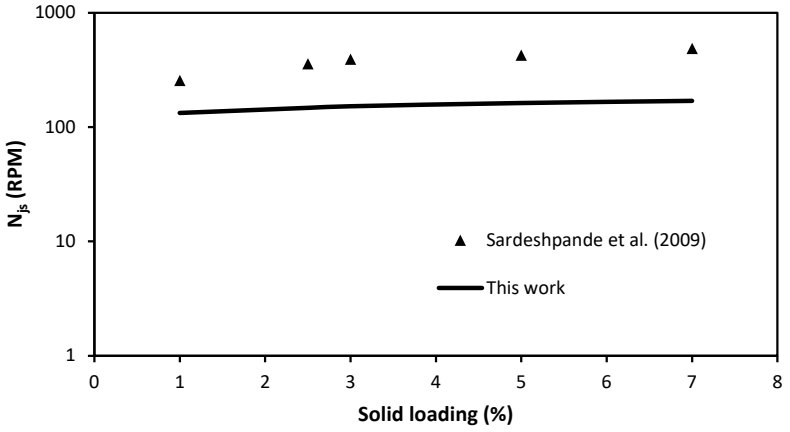

Fig. 7. Prediction of just suspended impeller speed versus published measurement.

3.5 Relationship between the mixing time and N_{js}

The impeller power draw is governed by several key parameters, including fluid density, power number, impeller diameter, and impeller speed. Under fully turbulent flow conditions, the impeller power number (N_{Po}) is expected to remain constant, reflecting the independence of power draw from viscosity in this regime. However, in practice, slight deviations from constant N_{Po} can occur due to variations in impeller geometry and design efficiency.

The critical impeller speed for just-suspended solids, denoted as N_{js}, is influenced by multiple factors: liquid viscosity, the density difference between solid and liquid phases, impeller speed, solids concentration (particle loading), particle size, and impeller diameter. Unlike general mixing performance, which depends strongly on power per unit volume, N_{js} emphasizes the balance between hydrodynamic forces and particle settling tendencies.

Mixing time, on the other hand, is primarily controlled by the power draw per unit volume and the geometrical ratios of tank and impeller diameter. The power input in a stirred tank

scales with the cube of the impeller speed (N^3) and the fifth power of the impeller diameter (D^5). This strong dependence indicates that increasing either impeller speed or diameter enhances both mixing time efficiency and the extent of solid dispersion.

It is important to note that the impeller speed corresponding to N_{js} is typically much lower than the speed required to achieve rapid mixing. This is because N_{js} does not directly scale with power per unit volume, whereas mixing time is highly sensitive to the energy input into the system.

Prediction of just-suspended impeller speed in solid-liquid stirred tank remain challenging. Even in the case when a reasonable prediction of flow field, power draw, and mixing time, prediction of just-suspended impeller is still somewhat poor. This issue needs to be taken into consideration when using CFD to predict the N_{js} of solid-liquid stirred tank.

4 Conclusion

A computational fluid dynamics (CFD) model for a solid–liquid stirred tank agitated by a pitched blade impeller was successfully developed and validated. The model can predict both the impeller power number and mixing time with good accuracy, showing only about 6–8% deviation from published experimental data. Furthermore, the predicted velocity vectors and the peak velocity magnitude in the impeller region are in close agreement with particle image velocimetry (PIV) measurements reported in the literature. This strong correlation demonstrates that the CFD model is capable of reliably capturing the complex flow field and hydrodynamic characteristics of solid–liquid mixing systems, and therefore can be used with confidence to evaluate and optimize stirred tank performance.

Acknowledgement

We acknowledge the funding from the Ministry of Higher Education Malaysia (FRGS/1/2018/TK02/UMP/02/17) with UMPSA reference RDU190145 and Research and Innovation Department of Universiti Malaysia Pahang Al-Sultan Abdullah.

References

1. C.D. Rielly, M.B. Habib, J. Sherlock, *Chem. Eng. Res. Des.* **85**, 953-962 (2007).
2. L. Li, B. Xu, *Chin. J. Mech. Eng.* **30**, 118–126 (2017).
3. A. Ochieng, M.S. Onyango, *Chem. Ind. Chem. Eng. Q*. **16**(4), 379-386 (2010).
4. A. Reid, R. Rossi, C. Cottini, A. Benassi, *Meccanica* **60**, 1613–1637 (2025).
5. Tamburini, A., Cipollina, A., Micale, G., Brucato, A., & Ciofalo, M. *Chem. Eng. J.* **193**, 234-255 (2012).
6. C. Sirasitthichoke, B. Teoman, J. Thomas, P.M. Armenante, *Chem. Eng. Sci.* **251**, 117411 (2022).
7. S. O'Regan, P.J. Frawley, O. Shardt, *Comput. Fluids* **266**, 106053 (2023).
8. A. Tamburini, A. Brucato, A. Cipollina, G. Micale, M. Ciofalo, *Int. J. Nonlinear Sci. Numer. Simul.* **13**(6), 427-443 (2012).
9. S. Hosseini, D. Patel, F. Ein-Mozaffari, M. Mehrvar, *Ind. Eng Chem. Res*, **49**, 4426–4435 (2010).
10. M.V. Sardeshpande, A.R. Sagi, V.A. Juvekar, V.V. Ranade, *Ind. Eng Chem. Res*, **48**, 9713–9722 (2009).
11. T.H. Shih, W.W. Liou, A. Shabbir, Z. Yang, J. Zhu, *Comput. Fluids* **24**, 227-238 (1995).

12. J. Gimbun, S.Y. Liew, Z.K. Nagy, C.D. Rielly, *Chem. Prod. Proc. Model.* **11**, 205-216 (2016).
13. C.Y. Ge, J.J. Wang, X.P. Gu, L.F. Feng, *Chem. Eng. Res. Des.* **92**(6), 1027-1036 (2014).
14. P.Trindade Koyro, H. Lima de Moura, R. de Lima Amaral, L. Freitas de Lima e Freitas, A. Duarte Barbutti, J.R. Nunhez, G.J. de Castilho, *J. Braz. Soc. Mech. Sci. Eng.* **44**(9), 421 (2002).
15. K. Rutheford, S.M.S. Mahmoudi, K.C. Lee, M. Yianneskis, *Trans. Inst. Chem. Eng. A* **74**, 369-378, (1996).
16. D. Chapple, S.M. Kresta, A. Wall, A. Afacan, *Chem. Eng. Res. Des.* **80**(4), 364-372 (2002).
17. N. Kuzmanić, R. Žanetić, M. Akrap, *Chem. Eng. Process.* **47**(4), 663–669 (2008).